Anthropogenic iron deposition alters the ecosystem and carbon balance of the Indian Ocean over a centennial timescale

Anh L. D. Pham[1,2] and Takamitsu Ito[1]

[1]School of Earth and Atmospheric Sciences, Georgia Institute of Technology, Atlanta Georgia U.S.A.
[2]Now at Laboratoire dOcanographie et de Climatologie: Exprimentation et Approches Numriques (LOCEAN), IPSL, CNRS/UPMC/IRD/MNHN, Paris, France

Key Points:

- Ecosystem dynamics controls the centennial impacts of anthropogenic nutrient deposition on the Indian Ocean carbon cycling.
- Diatom in the southeastern tropics and poleward of 50°S is stimulated by the anthropogenic iron, increasing the carbon uptake.
- Coccolithophores increases in the south Arabian Sea, weakening the carbon uptake there.

Corresponding author: Anh L. D. Pham, `anh.pham@eas.gatech.edu`

Abstract

Phytoplankton growth in the Indian Ocean is generally limited by macronutrients (nitrogen: N and phosphorus: P) in the north and by micronutrient (iron: Fe) in the south. Increasing atmospheric deposition of N and dissolved Fe (dFe) into the ocean due to human activities can thus lead to significant responses from both the northern and southern Indian Ocean ecosystems. Previous modeling studies investigated the impacts of anthropogenic nutrient deposition on the ocean, but their results are uncertain due to incomplete representations of the Fe cycling. This study uses a state-of-the-art ocean ecosystem and Fe cycling model to evaluate the transient responses of ocean productivity and carbon uptake in the Indian Ocean, focusing on the centennial time scale. The model includes three major dFe sources and represents an internal Fe cycling modulated by scavenging, desorption, and complexation with multiple, spatially varying ligand classes. Sensitivity simulations show that after a century of anthropogenic deposition, increased dFe input stimulates diatom productivity in the southern Indian Ocean poleward of 50°S and the southeastern tropics. However, diatom production weakens in the south of the Arabian Sea due to the P limitation, and diatom is outcompeted there by coccolithophores and picoplankton, which have a lower P demand. These changes in diatom and coccolithophores productions alter the balance between the organic and carbonate pumps in the Indian Ocean, increasing the carbon uptake in the south of 50°S and the southeastern tropics while decreasing it in the Arabian Sea. Our results reveal the important role of ecosystem dynamics in controlling the sensitivity of carbon fluxes in the Indian Ocean under the impact of anthropogenic nutrient deposition over a centennial timescale.

Plain Language Summary

Human activities have been intensifying the atmospheric nutrient input into the Indian Ocean where the marine ecosystem is diverse and biogeochemical features are complex. Thus, the response of the marine ecosystem in this region to the anthropogenic nutrient deposition can be significant. Results from previous studies on this topic are uncertain due to our limited understanding of the ocean micronutrient, iron. In this paper, we address this issue through a suite of computer simulations with an improved iron cycling model. We found that after a century of anthropogenic deposition, the ocean carbon uptake is enhanced in the southeastern tropics of the Indian Ocean but decreases in the Arabian Sea because the ecosystem shifts towards organisms that produce calcite.

Taken together, these changes lead to a slight increase in the total carbon dioxide uptake in the Indian Ocean.

1 Introduction

The Indian Ocean accounts for around one-fifth of the ocean net primary production (Behrenfeld & Falkowski, 1997a) and contains two of the largest oxygen (O_2) minimum zones (OMZs) of the world oceans in the northern part (the Arabian Sea and the Bay of Bengal) (Stramma et al., 2010). In these two regions, phytoplankton growth is generally limited by macronutrients because of the relatively shallow mixed layer and the Ekman downwelling that transports nutrients away from the euphotic layer. Furthermore, the low O_2 water in the OMZs promote nitrogen (N) loss through denitrification (Moore et al., 2013; Wang et al., 2019). In the northern Indian Ocean, the concentration of dissolved iron (dFe) is relatively high ($\sim$ 0.6 nM in the surface and $\sim$ 1.5 nM in the subsurface 200-1000m water) due to relatively high dFe inputs from atmospheric deposition and reduced sediments over the continental shelves (Nishioka et al., 2013; Chinni et al., 2019). However, Fe can still be a limiting factor for the nitrogen-fixer diazotrophs, which have a higher demand for Fe than other phytoplankton (Moore et al., 2013; Moffett et al., 2015). In contrast, the southern part of the Indian Ocean shows a very low dFe concentration ($\sim$ 0.2 nM), indicating that the biological productivity in this region can be Fe-limited (Nishioka et al., 2013; Chinni et al., 2019). These contrasting biogeochemical regimes between different parts of the Indian Ocean imply a diverse and complex response of the marine ecosystem to perturbations. Atmospheric deposition of N and dFe into the Indian Ocean has been increasing due to human activities, which including burning of fossil fuels, agriculture, and land use changes (Mahowald et al., 2009; Duce et al., 2008; Baker et al., 2017). Human activities also emit anthropogenic aerosols, which modify mobilization processes and atmospheric processing. Atmospheric dust deposition, which is generally stronger in the northern Indian Ocean, provides a direct input of bioavailable N, potentially relieving the macronutrient limitation. Increased atmospheric deposition can also provide dFe to support the growth of diazotrophs, and the deposited dFe can be transported to the southern part of the Indian Ocean (Boyd & Tagliabue, 2015). In general, a significant response of the Indian Ocean ecosystem to anthropogenic deposition from the atmosphere is expected, including a higher organic carbon export flux, stronger O_2 demand, thus an increase of the ocean carbon uptake and an expansion of OMZs (Moffett et al., 2015).

Recent modeling studies have examined the impact of anthropogenic nutrient deposition into the ocean by driving ocean biogeochemistry models with atmospheric deposition fields derived from atmospheric chemical transport models (Krishnamurthy et al., 2009, 2007; Ito et al., 2016; Guieu et al., 2019). These studies concluded that increasing dFe and N inputs stimulate marine nitrogen fixation in the subtropical North and South Pacific, enhance the primary production and export in the high-nutrient low-chlorophyll (HNLC) regions (Krishnamurthy et al., 2009), and accelerate the O_2 consumption in the tropical Pacific Ocean (Ito et al., 2016). Concurrently, the data coverage of dFe and other trace metal species expanded significantly thanks to the GEOTRACES program (Mawji et al., 2015; Schlitzer et al., 2018). The new observations revealed shortcomings of the earlier generations of the Fe cycling models, which did not include all of the dFe sources such as hydrothermal vents. Also, earlier models typically assumed a single ligand class with a uniform distribution. Thus, results from these earlier studies can contain significant uncertainty (Tagliabue et al., 2016). Significant model biases have been identified relative to the observed pattern of dFe revealed by the recent GEOTRACES observations (Mawji et al., 2015; Schlitzer et al., 2018). Models with constant ligand concentrations may underestimate the feedback between biological activity, ligand production, and dFe concentration to environmental changes (Völker & Tagliabue, 2015). Furthermore, impacts of anthropogenic atmospheric deposition on the Indian Ocean, where the nutrient cycling is complex and the phytoplankton community is diverse, has not been examined thoroughly and systematically. This paper aims to investigate the impact of increasing anthropogenic atmospheric N and dFe deposition on nutrient distribution, phytoplankton productivity, and the ocean carbon uptake in the Indian Ocean. We focus on the response of the ocean ecosystem over a timescale of 100 years, which is important to human activities and policy decisions. To this end, we use an ocean ecosystem model, which represents major phytoplankton types (Dutkiewicz et al., 2014), coupled with a recently improved Fe cycling scheme (Pham & Ito, 2018, 2019). The Fe scheme includes many crucial processes controlling the ocean Fe cycling and demonstrated improvements in the representation of dFe distribution as observed by the GEOTRACES cruises. The ecosystem model has been used in several previous studies on examining the ocean biogeochemistry response to human perturbations (Dutkiewicz et al., 2014,

2013) and the interplay between different bigeochemical processes shaping the phytoplankton community structure (Dutkiewicz et al., 2012). Atmospheric deposition of dFe and N are derived from the three-dimensional atmospheric chemical transport model GEOS-Chem coupled with a comprehensive dust-Fe dissolution scheme (Ito et al., 2016; Johnson & Meskhidze, 2013). The rest of the paper is organized as follows. In section 2, we describe the model configuration and the experimental design. In section 3, we present results of sensitivity experiments. In section 4, we summarize the results and discuss their implications.

2 Model configuration and experimental design

The ocean model used in this study was based on the Massachusetts Institute of Technology general circulation model (Marshall, Hill, et al., 1997; Marshall, Adcroft, et al., 1997, MITgcm) with a biogeochemistry and ecosystem component (Dutkiewicz et al., 2014, 2012). The model domain was configured for a 2.8°x 2.8°horizontal grid spacing, and 23 vertical z-levels with grid spacing ranging from 10 m in the surface to 500 m at 5000 m. Ocean boundary layer physics was parameterized using the K-Profile Parameterization scheme (Large et al., 1994), and the effects of mesoscale eddies was parameterized using the isopycnal tracer and thickness diffusion scheme (Gent & Mcwilliams, 1990). The physical ocean circulation was forced by climatological wind and buoyancy forcing derived from the National Center for Environmental Prediction Reanalysis product (Kalnay et al., 1996).

The biogeochemical component of the model was based on Dutkiewicz et al. (2014), including the cycling of carbon (C), P, N, silica (Si), Fe and O_2 through inorganic, living, dissolved, and particulate organic phases. Two grazers and six phytoplankton types (diatom, coccolithophores, large eukaryotes, *prochlorococcus*, other pico-phytoplankton, and diazotrophs) were represented in the model. The phytoplankton growth rate was a function of the Chlorophyll: C ratio, temperature, light, and nutrient availability, following Hickman et al. (2010); Geider et al. (1998).

The refined Fe scheme, which were developed and documented in our recent publications (Pham & Ito, 2018, 2019), encompassed various important processes in the ocean Fe cycling. These processes included external dFe inputs from dust deposition, continental shelves, and hydrothermal vents. The model internal cycling of Fe considered scavenging of dFe onto and release of dFe from organic and lithogenic particles and dFe retention by spatially varying organic ligands. Scavenging of free dFe (Fe'), which is not bound to ligands, by organic particles was parameterized as a function of the concentrations of particulate organic matter and of Fe'. dFe scavenged by this process can be released back to the water column through the remineralization of sinking organic particles (Boyd et al., 2010). Different from the model used in previous publications (Pham & Ito, 2018, 2019), particulate organic matter is a prognostic variable in this model, and therefore its vertical attenuation with depth was explicitly calculated. As in Pham and Ito (2018, 2019), the inorganic scavenging process was parameterized as a first order loss process with a rate constant, k_{inorg}. This rate constant can significantly increase under the dust plume where elevated dust deposition increases the lithogenic particle concentration (Ye & Völker, 2017). This mechanism was represented in the model by scaling k_{inorg} with the atmospheric dFe flux. Scavenged dFe through this mechanism can also return to the water column by desorption from sinking particles. This return dFe flux was calculated from the vertical profile of sinking inorganic scavenged-Fe flux, which was represented by a power function with a coefficient of -0.4 (Pham & Ito, 2019). Atmospheric deposition fields of N and dFe were taken from the output of atmospheric chemical transport model GEOS-Chem (Johnson & Meskhidze, 2013). Anthropogenic effects on N and dFe deposition were calculated using the emission inventories for the year 2009, and the pre-industrial fluxes were calculated by turning off all anthropogenic emission sources. Details on this model and on how the industrial fluxes were calculated based on anthropogenic emission were described in Ito et al. (2016); Johnson and Meskhidze (2013).

The model was first spun up under the pre-industrial deposition of N and dFe for 1,000 years (*PreIn* run). Initialized from the last time step of the *PreIn* run, an additional integration was performed using the anthropogenic deposition of N and dFe. The model was further integrated for 1,000 years to achieve new quasi-steady states, but we only analyzed the response of the ecosystem and carbon cycle to the anthropogenic deposition during the first 100 years. This experiment was intended to examine the centennial impacts of anthropogenic N and dFe deposition on the Indian Ocean. In reality, there could be transient perturbations to the marine ecosystem and biogeochemistry on all timescales, including the effects of warming and increased stratification, circulation changes, riverine nutrient input, and acidification. Account for all these changes are beyond the scope of this paper. As a first step, we focused on a single perturbation in the atmospheric nutrient deposition to better understand the response to this particular anthropogenic forcing. In summary, model experiments were set up as follows:

- "*PreIn*" run forced by the pre-industrial atmospheric dFe and N deposition fields
- "*Ind*" run forced by the contemporary atmospheric dFe and N deposition fields

Results from the *Ind* run were analyzed by comparing the differences in nutrient fields, biological productivity, phytoplankton community structure, and carbon uptake, all in relation to the *PreIn* run.

3 Results

3.1 Model validation

We first evaluated the model performance and its ability to reproduce major biogeochemical features of the Indian Ocean by comparing the observed, modern distributions of nutrient tracers with the equilibrium state of the *Ind* model run, which is forced by contemporary forcings.

Biological productivity is influenced by the nutrient distributions, thus it is essential that the model captures the nutrient fields well. First, we examined the model nitrate (NO_3^-) distribution using the World Ocean Atlas (Garcia et al., 2014) as the observational benchmark (Figure 1a). The model is certainly not perfect as it underestimated the NO_3- concentrations at high latitudes. However, the general pattern of the near-surface NO_3- distribution was captured reasonably well (Figure 1b). When compared to the World Ocean Atlas, the model reproduced the boundary between the low and high concentration approximately at 40°S.

Next, we examined the meridional transect of dFe along the GEOTRACES line GI04 (Schlitzer et al., 2018), focusing on the upper ocean (0-1000m). dFe in the upper ocean is more important for sustaining biological productivity, which mainly occurs in the euphotic zone. The model captured the pattern of dFe remarkably well especially in the top 1,000m, in consistent with results shown by Pham and Ito (2018) (Figure 1de). Specifically, it captured the strong meridional gradient of dFe centered at around 10°S where the observed dFe concentration is high (0.8 - 1.3 nM) in the subsurface water of the tropical thermocline but it is very low in the southern part ($\sim$ 0.2 nM). The model also re-

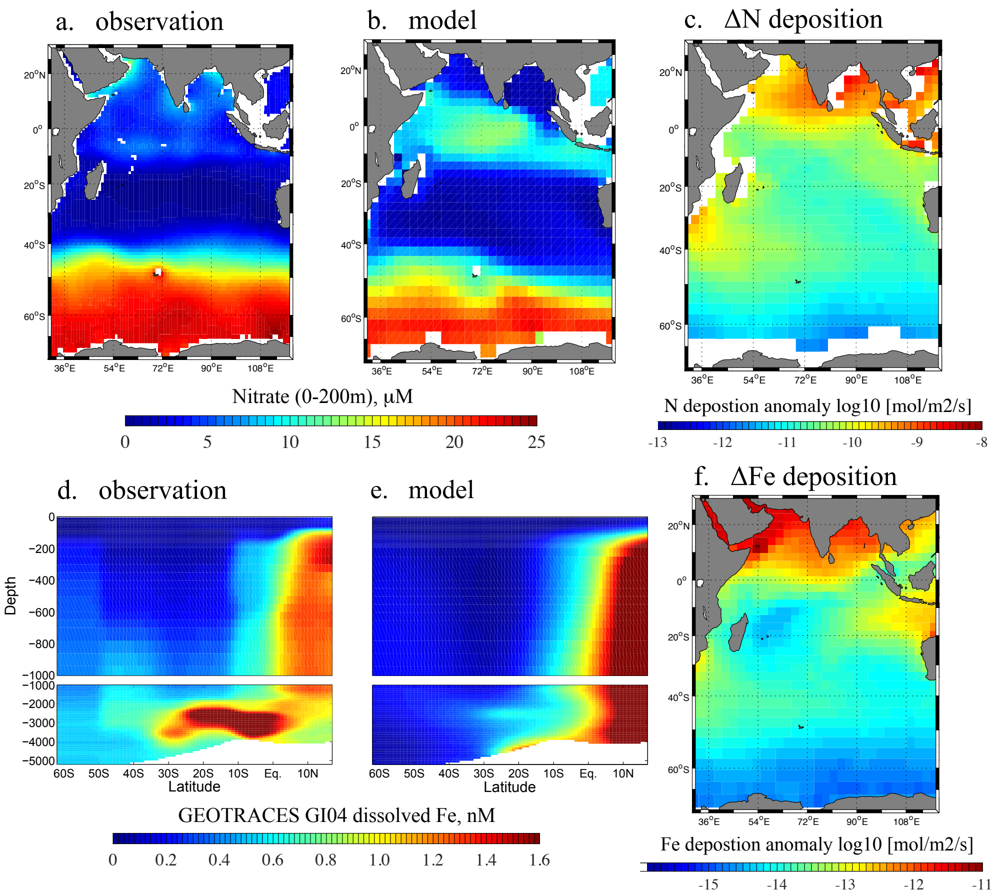

Figure 1. Upper panel (a): World Ocean Atlas Annual Mean NO_3^- averaged over the top 200 m, (b): Mean modeled NO_3^- averaged over the top 200 m ocean - results from the *Ind* run, Lower panel (c) Atmospheric deposition anomaly (*Ind* run - *PreIn* run) of fixed N into the surface of the Indian Ocean used in this study, (d): Observed dFe concentration from the GEOTRACES program along the Indian Ocean GI04 transect, (e) dFe concentration - results from the *Ind* run - along the Indian Ocean GI04 transect, and (f) atmospheric deposition anomaly (*Ind* run - *PreIn* run) of dFe into the surface of the Indian Ocean

produced the subsurface peak of dFe in the northern Arabian Sea ($\sim 10°$N) and the strong vertical gradient in the dFe concentration observed there between the surface (0-200m) and subsurface waters ($>$ 200m). The only major bias in this model is the underestimation of hydrothermal signal around the Central Indian Ridge segment. This is likely because our model did not represent the unique interaction between particulate and dissolved phases of Fe released from the vents, which supports the lateral transport of dFe away from the vent sources (Fitzsimmons et al., 2017). Moreover, measurements by Fitzsimmons et al. (2017) show that a large portion of dFe released from hydrothermal vents can be nanoparticles of pyrite or Fe(III) oxides, which are not represented in the model.

When compared with the zonal mean of the satellite-derived annual mean net primary production (NPP) averaged from 2003 to 2016 (Behrenfeld & Falkowski, 1997b) in the Indian Ocean (Figure S1), our model showed an underestimation for NPP in the subtropics and in the southern Indian Ocean (south of $\sim 20°$S). This is a common deficiency of coarse-resolution ocean ecosystem models (Dutkiewicz et al., 2014, 2013, 2012), which do not adequately represent the coastal current systems and open ocean eddies. Without these small-scale processes, the model is missing important nutrient sources and tend to underestimate the biological productivity near the coasts and in the Southern Ocean. However, our model captured the patterns of the observed NPP in the tropics (north of 10°S) reasonably well. Since the NPP is an important indicator of the ocean organic carbon pumps, it is encouraging that our model started representing some features despite its low spatial resolution. The biases shown in Figure S1 indicate that our model might underestimate the biological carbon pumps in the subtropical and mid-latitude Indian Ocean.

3.2 Sensitivity experiments

The increase in the atmospheric deposition of fixed N and dFe into the Indian Ocean is shown in Figure 1cf). A large increase in the dFe deposition occurred in the coastal regions of the northern Indian Ocean and north of Australia, while it moderately increased over the equatorial and southern regions. Integrating over the Indian Ocean (30°E-110°E, 80°S-30°N), the dFe flux increased from 38.78 mol/s to 87.78 mol/s, more than doubling the pre-industrial deposition. N deposition exhibited a similar spatial pattern to dFe. Again integrating over the Indian Ocean, the fixed N flux increased from $6.3 \cdot 10^3$ mol/s to $1.3 \cdot 10^4$ mol/s, approximately doubling from its pre-industrial value.

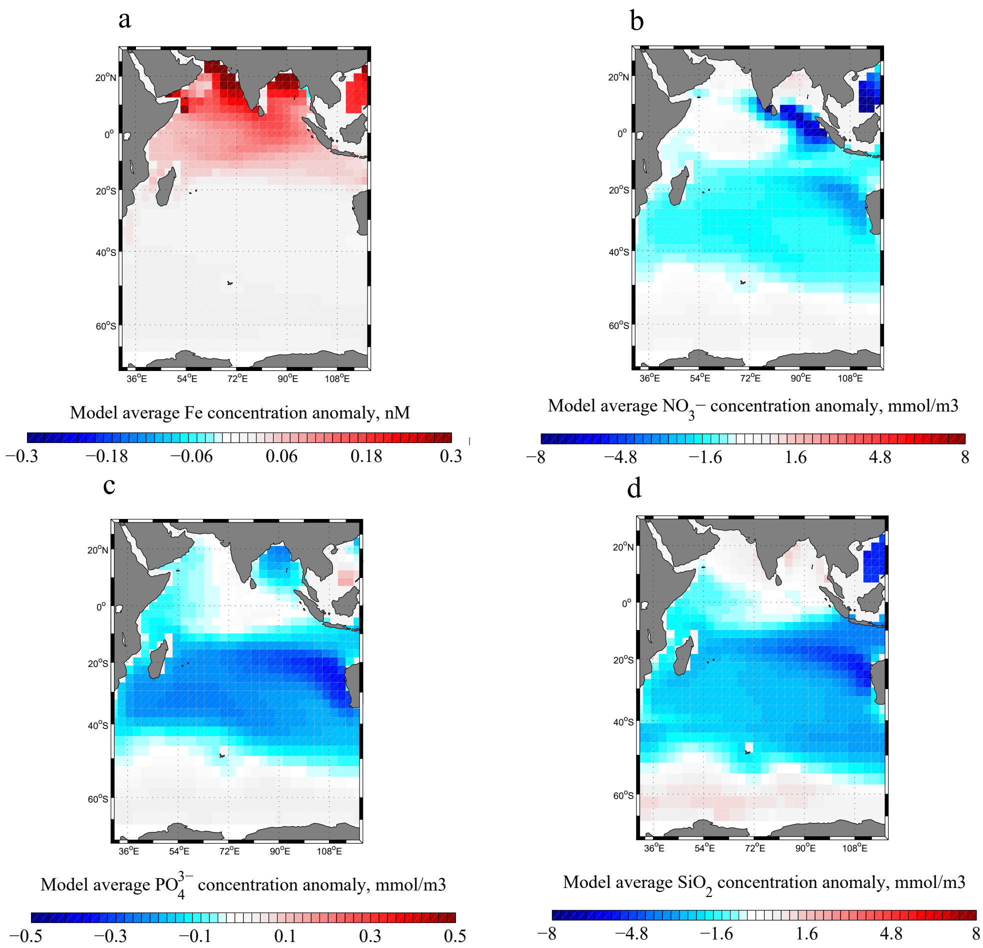

Figure 2. Model(*Ind* run) concentration anomaly relative to the *PreIn* run averaged from 0-300m in the Indian Ocean for (a) dFe, (b) nitrate (NO_3^-), (c) phosphate (PO_4^{3-} and (d) silicate (SiO_2) after 100 years of being forced under the anthropogenic N and Fe depositions

Comparing *PreIn* and *Ind* runs, the response of the dFe concentration for the upper 300m ocean after 100 years of anthropogenic deposition was an increase of approximately 0.3nM in the northern Indian Ocean, whereas the response was much weaker poleward of 20°S (Figure 2a). This pattern was generally similar to the atmospheric deposition of dFe where the northern Indian Ocean received more anthropogenic dFe deposition relative to the Southern Ocean by several orders of magnitude. In contrast, the response of the near-surface NO_3^- (Figure 2b) was very different from the atmospheric deposition pattern. NO_3^- concentration generally decreased in the Indian Ocean even though the ocean received more N from atmospheric deposition. In particular, the N decrease was significant in the subtropical region between 20°and 40°S. There was also a region of significant N decrease in the Bay of Bengal. This changes in the upper 300m NO_3- concentration implies that the biological N uptake was enhanced in many parts of the Indian Ocean. Other macro nutrients (P and Si) also decreased with the same pattern (Figure 2cd). The P decrease was widespread and more enhanced in the Bay of Bengal and in the subtropics between 20°- 40°S. The decline of macronutrients between 20°- 40°S suggests that the increased Fe and N atmospheric deposition altered the productivity there even though the anthropogenic deposition was relatively weak in these region and dFe concentration was close to be depleted.

In Figure 3, we showed changes in two major phytoplankton groups: diatom and coccolithophores although the model includes six phytoplankton types. This is because the majority of changes in the total primary production and ocean carbon uptake can be explained by changes in the diatom and coccolithophores. Supplementary Figure S2 shows changes in the other four phytoplankton species for a complete description. In brief, the increased dFe deposition stimulated the growth of nitrogen-fixer diazotrophs in the Bay of Bengal (Figure S2). In contrast, diazotrophs concentration decreased in the northern Arabian Sea together with coccolithophores, likely due to more intense P limitation in this region, which ultimately limited phytoplankton growth.

Diatom concentration increased significantly in the south of 40°S, in the Bay of Bengal, and in the southeastern tropics, which are close to the regions of decrease in N, P, and Si (Figure 2). Diatom is the only phytoplankton type that utilizes Si, therefore the decrease of Si confirms the role played by diatom in these regions. In contrast, diatom concentrations weakened in the southern part of the Arabian Sea and slightly decreased along 40°S close to regions having an increase in the coccolithophores (Figure 3b) and

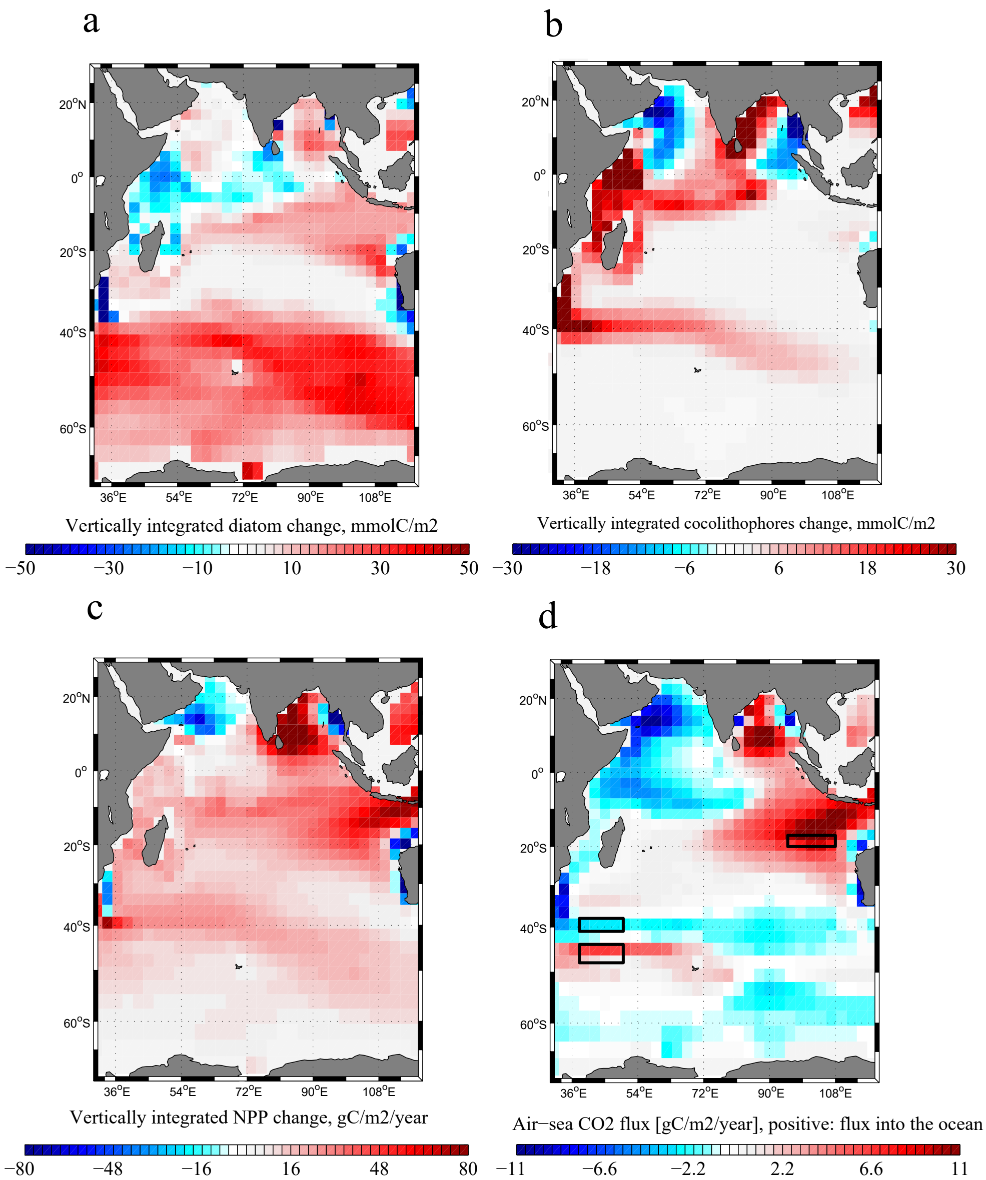

Figure 3. The vertically integrated anomaly between the *Ind* and the *PreIn* runs for (a) diatom concentration, (b) coccolithophores concentration, (c) primary production, and (d) air-sea CO_2 flux after 100 years of being forced under the anthropogenic N and Fe depositions. All phytoplankton biomass is measured in the units of P in the model. The air-sea CO_2 flux is positive into the ocean. The three black boxes shown in (d) are three regions where we will further analyze the evolution of changes in the phytoplankton community and air-sea CO_2 flux during the first 100 years after being forced by anthropogenic deposition.

picoplankton (small phytoplankton) concentrations (Figure S2b). These changes indicate that diatom was out-competed in these regions by coccolithophores and picoplankton. One explanation for these changes is that diatom has a faster maximum growth rate but requires a higher P concentration relative to coccolithophores and picoplankton (Riegman et al., 2000). Thus, the decrease in P supply along 40°S and in the southern part of the Arabian Sea caused diatom to be less competitive and helped coccolithophores become more dominant. In addition, diatom poleward of 40°S was relieved from Fe limitation and consumed more Si, therefore decreasing the Si transport equatorward and making diatom become Si-limited in the low latitudes.

The competition between diatoms and coccolithophores in the southern part of the Arabian Sea and along 40°S caused a shift in the biological carbon pump in these regions from organic to calcium carbonate pumps. An increase in coccolithophores and decrease in diatom decreased the surface alkalinity relative to dissolved inorganic carbon (DIC). Production of calcium carbonate shells consumes calcium ion in the surface water, leading to a loss of alkalinity. In turn, the decrease in surface alkalinity shifted the carbonate chemistry of this region towards a more acidic condition with a lower pH. The ability of seawater to retain inorganic carbon decreases with a lower pH, leading to an increase in the partial pressure of $\mathrm{CO_2}$ ($\mathrm{pCO_2}$). Consequently, it decreased the rate of ocean CO_2 uptake along 40°S and in the Arabian Sea (Figure 3d). This is somewhat counterintuitive because the primary productivity indeed increased along 40°S and in the Southern Arabian sea under the modern atmospheric deposition. However, the intensified carbonate pump led to a decrease in the regional ocean carbon uptake. In contrast, the increase in diatom productivity in the south of 40°S, the Bay of Bengal, and the southeastern tropical Indian Ocean contributed to a stronger organic carbon pump, thus increasing the ocean CO_2 uptake (Figure 3d).

We further analyzed the evolution of changes in the phytoplankton community and air-sea CO_2 flux during the first 100 years after being forced by anthropogenic deposition (Figure 4) in three regions shown in Figure 3d. These three regions include the southeastern tropics (SE tropics) and the regions along 40°S and 50°S in the south western Indian Ocean, close to the Agulhas current (Agulhas 40°S and Agulhas 50°S). In particular, we examined the evolution of changes during the first 100 years for diatom (red lines) and coccolithophores (blue lines) concentrations, NPP (green lines), and air-sea CO_2 flux (black lines). These three regions showed a contrasting response in the ocean

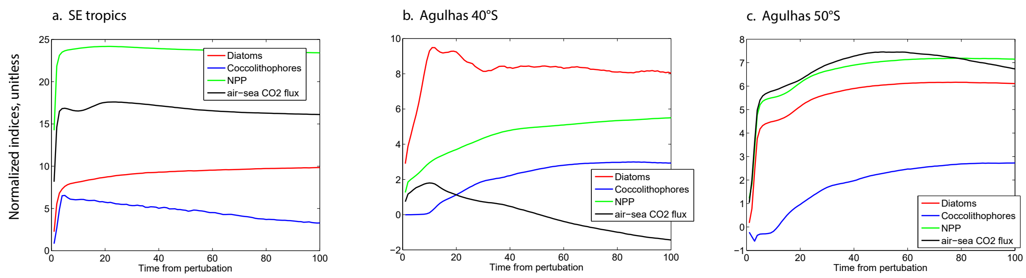

Figure 4. (a) The changes in the concentration of diatom (red lines), coccolithophores (blue lines), NPP (green lines), and the air-sea CO_2 flux (black lines) summed over the regions defined in Figure 3. (a) the southeastern (SE) tropics, (b) the Agulhas 40°S, (c) the Agulhas 50°S. All the changes in phytoplankton biomass and carbon uptake were normalized by dividing the change in each quantity by its standard deviation

CO_2 uptake flux even though their NPP all increased significantly after 100 years of being forced under the modern atmospheric deposition.

All the anomalies shown in Figure 4 were normalized (divided by the standard deviation) to facilitate the comparison between different quantities. In the SE tropics, diatom and coccolithophores concentrations both rapidly increased during the first 10 years under the anthropogenic deposition, which led to an increase in the regional NPP and ocean CO_2 uptake. However, coccolithophores steadily decreased after this initial increase, whereas diatom kept growing. In this region, the effect of diatom increase dominated, leading to an increase in the NPP and the ocean CO_2 uptake after 100 years.

In contrast, coccolithophores in the Agulhas 40°S steadily increased over the 100-year time-frame, while diatom significantly enhanced during the first 10 years, then slightly decreased and stayed relative stable after 20 years. The increase in coccolithophores started dominating after around 20 years, which caused a decreasing trend of the air-sea CO_2 flux despite a continued increase in the NPP. After ∼50 years, the air-sea CO_2 flux changed its sign and this region became a source of carbon to the atmosphere.

The centennial evolution of phytoplankton community in the Agulhas 50°S is different than the other two regions. Both diatom and coccolithophores increased significantly, thus enhancing the primary production. The impact of enhanced diatom growth dominated in this region, which led to an increase in the ocean carbon uptake. In summary, our analysis here further demonstrated the compensation between the effects of growing diatom and coccolithophores, which controls the organic and calcium carbonate carbon pumps, ultimately determining the air-sea CO_2 flux.

4 Discussion and Conclusion

Human activities have heavily perturbed atmospheric deposition of dFe and N into the ocean since the start of the industrial era (Mahowald et al., 2017, 2009). This has a crucial consequence to the marine ecosystem especially in regions where phytoplankton growth is limited by the availability of these nutrients, such as the oligotrophic regions limited by N and/or P and the HNLC regions limited by Fe. Earlier modeling studies estimated a modest response of the ocean primary production and air-sea CO_2 exchange to the anthropogenic nutrient deposition at the global scale, but also predicted striking responses of biogeochemical cycles at regional scales (Krishnamurthy et al., 2007, 2009; Ito et al., 2016; Somes et al., 2016). Specifically, Krishnamurthy et al. (2009) suggested that increasing N and dFe inputs stimulate marine nitrogen fixation in the subtropical North and South Pacific where Fe limitation of diazotrophs is relieved but decrease it in the Indian Ocean where diazotrophs become more P limited.

This study focused on the centennial response of the Indian Ocean ecosystem and carbon cycle to increased atmospheric nutrient inputs caused by the anthropogenic effects on aerosol deposition. We used a state-the-art ocean ecosystem and Fe cycling model, constrained by the new high-quality data of Fe from the GEOTRACES program (Mawji et al., 2015; Schlitzer et al., 2018). This new dataset puts a much more stringent constraint on the representation of Fe cycling in the ocean biogeochemistry models, thereby improving our process-level understanding and quantification of key processes (Tagliabue et al., 2016, 2017). Our ocean model, when forced under the contemporary deposition (evaluated at year 2009), was able to reproduce many important features of the observed nutrient distributions and some important patterns of the NPP. Although the model still showed some biases, it captured major aspects of the subsurface dFe pattern along the Indian Ocean GI04 transect remarkably well. Model experiments were designed to examine the centennial impacts of anthropogenic N and dFe deposition, separated from the other anthropogenic and natural drivers, such that we can clearly understand the mechanisms at play at a timescale that is relevant for human activities and policies. Of course, several different types of perturbations affect marine ecosystems and their biogeochemistry since the industrial revolution, including ocean warming, ocean circulation changes, riverine nutrient input, and acidification due to the uptake of fossil fuel CO_2. Among these perturbations, the anthropogenic nutrient input from rivers can provide a significant amount of N and P to the open ocean (Sharples et al., 2017). Thus, if this input were included in the model, the phytoplankton community in the northern Indian Ocean could be relieved of P-limitation, and therefore could be significantly enhanced. Nevertheless, a comprehensive analysis of the realistic, transient ecosystem changes is beyond the scope of this paper. Even in this idealized experiment, the response of ecosystems and the carbon cycle was complex and exhibited unique spatial patterns.

The atmospheric fluxes of N and dFe into the Indian Ocean both doubled their values since the industrial revolution due to anthropogenic effects. Due to this significant increase in the nutrient deposition, the net primary production summed up over the whole basin increased $\sim 21\%$, (see Table 1). However, the ocean CO_2 uptake only slightly increased by 1% if integrated over the Indian Ocean. This slight increase in the ocean CO_2 uptake despite the significant increase in the NPP can be explained by analyzing changes in the ocean CO_2 uptake pattern and phytoplankton community structure, which did not respond uniformly under the anthropogenic deposition. In particular, productivity and carbon uptake both intensified along 50 °S and in the southeastern tropics. These changes were influenced by the increasing diatom productivity and a stronger organic carbon pump. In contrast, the northern Arabian Sea exhibited decreased productivity and a weaker carbon uptake due to the intensification of P limitation. An increase in coccolithophores production along 40°S and in the southern Arabian Sea led to a stronger calcium carbonate pump at the expense of diatom productivity. This caused the ocean carbon uptake to weaken even though the local primary productivity increased. It should be noted that our model underestimated the vertically-integrated NPP relative to satellite-based observations, which could lead to biases in the air-sea CO_2 response. The biases in NPP is mostly in the mid-latitude and southern part of the Indian Ocean (south of 20°S) where the current model's coarse resolution could not represent the coastal current systems and eddies adequately. Despite this caveat, our results suggest that the regional pattern of responses in the NPP and ocean carbon uptake to anthropogenic forcings can be much more complicated than a simple uniform increase, which is due to competitions within the phytoplankton community.

Table 1. The total primary production (PP) and air-sea CO_2 flux (positive values mean the ocean uptakes CO_2) over the Indian Ocean 30°E-110°E, 80°S-30°N

Model run	PP (PgC/year)	air-sea CO_2 flux (gC/year)
PreIn	4.75	0.282
Ind (After 100 yrs)	5.75	0.286

The Indian Ocean is an important region of the world ocean, containing a large volume of low O_2 water in the north where phytoplankton is limited by macronutrient (Stramma et al., 2010) and a HNLC region in the southern sector where biological productivity is limited by Fe (Twining et al., 2019). This diverse and complex region is vulnerable to an increase in atmospheric inputs of N and dFe due to industrial activities (Mahowald et al., 2009; Duce et al., 2008; Baker et al., 2017). Our results suggested that anthropogenic aerosol inputs may moderately increase the basin-scale productivity over a centennial timescale but may cause significant changes in the regional patterns of productivity and the composition of the phytoplankton community. The latter change can alter the functioning of the biological carbon pump with non-negligible impacts on the basin-scale patterns of carbon uptake. Previous studies have pointed to an increase in coccolithophores biomass under global warming and increasing CO_2 concentration with important consequences to the ocean calcification and global carbon cycle (Krumhardt et al., 2016; Krumhardt, Lovenduski, Iglesias-Rodriguez, & Kleypas, 2017; Krumhardt et al., 2019; Krumhardt, Lovenduski, Long, & Lindsay, 2017). We further emphasized the crucial role of this calcifier phytoplankton due to its sensitivity to nutrient inputs. In conclusion, our results suggested a complicated and strong, regional sensitivity of the ecosystem and carbon fluxes in the Indian Ocean under the impact of anthropogenic pollution.

Acknowledgments

The model outputs, relevant data, and MATLAB scripts to reproduce the figures shown in this manuscript are stored at Zenodo (https://doi.org/10.5281/zenodo.3866205). We acknowledge the GEOTRACES group for making the dissolved iron transect data publicly available in its website: http://www.egeotraces.org. We thank Stephanie Dutkiewicz and Martial Taillefert for providing helpful comments and suggestion. AP is grateful for the support by the ANR project CIGOEF (Grant number ANR-17-CE32-0008). TI is thankful for the funding support by the National Science Foundation (Grant number 1744755, 1737188).

References

Baker, A. R., Kanakidou, M., Altieri, K. E., Daskalakis, N., Okin, G. S., Myriokefalitakis, S., ... Prospero, J. M. (2017). Observation- and model-based estimates of particulate dry nitrogen deposition to the oceans [Journal Article]. *Atmos. Chem. Phys.*, *17*(13), 8189-8210. Retrieved from `https://www.atmos-chem-phys.net/17/8189/2017/` doi: 10.5194/acp-17-8189-2017

Behrenfeld, M. J., & Falkowski, P. G. (1997a). A consumer's guide to phytoplankton primary productivity models [Journal Article]. *Limnology and Oceanography*, *42*(7), 1479-1491. Retrieved from `http://dx.doi.org/10.4319/lo.1997.42.7.1479` doi: 10.4319/lo.1997.42.7.1479

Behrenfeld, M. J., & Falkowski, P. G. (1997b). Photosynthetic rates derived from satellite-based chlorophyll concentration [Journal Article]. *Limnology and Oceanography*, *42*(1), 1-20. Retrieved from `https://doi.org/10.4319/lo.1997.42.1.0001` doi: 10.4319/lo.1997.42.1.0001

Boyd, P. W., Ibisanmi, E., Sander, S. G., Hunter, K. A., & Jackson, G. A. (2010). Remineralization of upper ocean particles: Implications for iron biogeochemistry [Journal Article]. *Limnology and Oceanography*, *55*(3), 1271-1288. Retrieved from `http://dx.doi.org/10.4319/lo.2010.55.3.1271` doi: 10.4319/lo.2010.55.3.1271

Boyd, P. W., & Tagliabue, A. (2015). Using the l* concept to explore controls on the relationship between paired ligand and dissolved iron concentrations in the ocean [Journal Article]. *Marine Chemistry*, *173*, 52-66. Retrieved from `http://www.sciencedirect.com/science/article/pii/S0304420314002254` doi: http://dx.doi.org/10.1016/j.marchem.2014.12.003

Chinni, V., Singh, S. K., Bhushan, R., Rengarajan, R., & Sarma, V. (2019). Spatial variability in dissolved iron concentrations in the marginal and open waters of the indian ocean. *Marine Chemistry*, *208*, 11 - 28. Retrieved from `http://www.sciencedirect.com/science/article/pii/S0304420318300586` doi: https://doi.org/10.1016/j.marchem.2018.11.007

Duce, R. A., LaRoche, J., Altieri, K., Arrigo, K. R., Baker, A. R., Capone, D. G., ... Zamora, L. (2008). Impacts of atmospheric anthropogenic nitrogen on the open ocean [Journal Article]. *Science*, *320*(5878), 893-897. Retrieved from `https://science.sciencemag.org/content/sci/320/5878/893.full.pdf` doi: 10.1126/science.1150369

Dutkiewicz, S., Scott, J. R., & Follows, M. J. (2013). Winners and losers: Ecological and biogeochemical changes in a warming ocean [Journal Article]. *Global Biogeochemical Cycles*, *27*(2), 463-477. Retrieved from `https://agupubs.onlinelibrary.wiley.com/doi/abs/10.1002/gbc.20042` doi: 10.1002/gbc.20042

Dutkiewicz, S., Ward, B. A., Monteiro, F., & Follows, M. J. (2012). Interconnection of nitrogen fixers and iron in the pacific ocean: Theory and numerical simulations [Journal Article]. *Global Biogeochemical Cycles*, *26*(1). Retrieved from `https://agupubs.onlinelibrary.wiley.com/doi/abs/10.1029/2011GB004039` doi: doi:10.1029/2011GB004039

Dutkiewicz, S., Ward, B. A., Scott, J. R., & Follows, M. J. (2014). Understanding predicted shifts in diazotroph biogeography using resource competition theory [Journal Article]. *Biogeosciences*, *11*(19), 5445-5461. Retrieved from `http://www.biogeosciences.net/11/5445/2014/` doi: 10.5194/bg-11-5445-2014

Fitzsimmons, J. N., John, S. G., Marsay, C. M., Hoffman, C. L., Nicholas, S. L., Toner, B. M., ... Sherrell, R. M. (2017). Iron persistence in a distal hydrothermal plume supported by dissolved-particulate exchange [Journal Article]. *Nature Geosci*, *advance online publication*. Retrieved from `http://dx.doi.org/10.1038/ngeo2900` doi: 10.1038/ngeo2900http://www.nature.com/ngeo/journal/vaop/ncurrent/abs/ngeo2900.html#supplementary-information

Garcia, H. E., Locarini, R., Boyer, T., Antono, J., Baranova, O., Zweng, M., ... Johnson, D. (2014). World ocean atlas 2013, volume 3: Dissolved oxygen, apparent oxygen utilization, and oxygen saturation [Journal Article]. *S. Levitus, Ed., A. Mishonov Technical Ed.;*, *3*, NOAA Atlas NESDIS 75, 27 pp.

Geider, R. J., Maclntyre, H. L., & Kana, T. M. (1998). A dynamic regulatory model of phytoplanktonic acclimation to light, nutrients, and temperature [Journal Article]. *Limnology and Oceanography*, *43*(4), 679-694. Retrieved from https://aslopubs.onlinelibrary.wiley.com/doi/abs/10.4319/lo.1998.43.4.0679 doi: 10.4319/lo.1998.43.4.0679

Gent, P. R., & Mcwilliams, J. C. (1990). Isopycnal mixing in ocean circulation models [Journal Article]. *Journal of Physical Oceanography*, *20*(1), 150-155. Retrieved from https://journals.ametsoc.org/doi/abs/10.1175/1520-0485%281990%29020%3C0150%3AIMIOCM%3E2.0.CO%3B2 doi: 10.1175/1520-0485(1990)020⟨0150:imiocm⟩2.0.co;2

Guieu, C., Al Azhar, M., Aumont, O., Mahowald, N., Levy, M., Ethé, C., & Lachkar, Z. (2019). Major impact of dust deposition on the productivity of the arabian sea [Journal Article]. *Geophysical Research Letters*, *46*(12), 6736-6744. Retrieved from https://agupubs.onlinelibrary.wiley.com/doi/abs/10.1029/2019GL082770 doi: 10.1029/2019gl082770

Hickman, A. E., Dutkiewicz, S., Williams, R. G., & Follows, M. J. (2010). Modelling the effects of chromatic adaptation on phytoplankton community structure in the oligotrophic ocean [Journal Article]. *Marine Ecology Progress Series*, *406*, 1-17. Retrieved from https://www.int-res.com/abstracts/meps/v406/p1-17/

Ito, T., Nenes, A., Johnson, M. S., Meskhidze, N., & Deutsch, C. (2016). Acceleration of oxygen decline in the tropical pacific over the past decades by aerosol pollutants [Journal Article]. *Nature Geosci*, *9*(6), 443-447. Retrieved from http://dx.doi.org/10.1038/ngeo2717 doi: 10.1038/ngeo2717http://www.nature.com/ngeo/journal/v9/n6/abs/ngeo2717.html#supplementary-information

Johnson, M. S., & Meskhidze, N. (2013). Atmospheric dissolved iron deposition to the global oceans: effects of oxalate-promoted fe dissolution, photochemical redox cycling, and dust mineralogy [Journal Article]. *Geosci. Model Dev.*, *6*(4), 1137-1155. Retrieved from http://www.geosci-model-dev.net/6/1137/2013/ doi: 10.5194/gmd-6-1137-2013

Kalnay, E., Kanamitsu, M., Kistler, R., Collins, W., Deaven, D., Gandin, L., ... Joseph, D. (1996). The ncep/ncar 40-year reanalysis project [Journal Article]. *Bulletin of the American Meteorological Society*, *77*(3), 437-472. Retrieved from https://doi.org/10.1175/1520-0477(1996)077<0437:TNYRP>2.0.CO;2 doi: 10.1175/1520-0477(1996)077⟨0437:TNYRP⟩2.0.CO;2

Krishnamurthy, A., Moore, J. K., Mahowald, N., Luo, C., Doney, S. C., Lindsay, K., & Zender, C. S. (2009). Impacts of increasing anthropogenic soluble iron and nitrogen deposition on ocean biogeochemistry [Journal Article]. *Global Biogeochemical Cycles*, *23*(3). Retrieved from https://agupubs.onlinelibrary.wiley.com/doi/abs/10.1029/2008GB003440 doi: 10.1029/2008gb003440

Krishnamurthy, A., Moore, J. K., Zender, C. S., & Luo, C. (2007). Effects of atmospheric inorganic nitrogen deposition on ocean biogeochemistry [Journal Article]. *Journal of Geophysical Research: Biogeosciences*, *112*(G2). Retrieved from https://agupubs.onlinelibrary.wiley.com/doi/abs/10.1029/2006JG000334 doi: 10.1029/2006jg000334

Krumhardt, K. M., Lovenduski, N. S., Freeman, N. M., & Bates, N. R. (2016). Apparent increase in coccolithophore abundance in the subtropical north atlantic from 1990 to 2014 [Journal Article]. *Biogeosciences*, *13*(4), 1163-1177. Retrieved from https://www.biogeosciences.net/13/1163/2016/ doi: 10.5194/bg-13-1163-2016

Krumhardt, K. M., Lovenduski, N. S., Iglesias-Rodriguez, M. D., & Kleypas, J. A. (2017). Coccolithophore growth and calcification in a changing ocean [Journal Article]. *Progress in Oceanography*, *159*, 276-295. Retrieved from http://www.sciencedirect.com/science/article/pii/S0079661117302148 doi: https://doi.org/10.1016/j.pocean.2017.10.007

Krumhardt, K. M., Lovenduski, N. S., Long, M. C., Levy, M., Lindsay, K., Moore, J. K., & Nissen, C. (2019). Coccolithophore growth and calcification in an acidified ocean: Insights from community earth system model simulations [Journal Article]. *Journal of Advances in Modeling Earth Systems*, *11*(5), 1418-1437. Retrieved from https://agupubs.onlinelibrary.wiley.com/doi/abs/10.1029/2018MS001483 doi: 10.1029/2018ms001483

Krumhardt, K. M., Lovenduski, N. S., Long, M. C., & Lindsay, K. (2017). Avoidable impacts of ocean warming on marine primary production: Insights from the cesm ensembles [Journal Article]. *Global Biogeochemical Cycles*, *31*(1), 114-133. Retrieved from https://agupubs.onlinelibrary.wiley.com/doi/abs/10.1002/2016GB005528 doi: 10.1002/2016gb005528

Large, W. G., McWilliams, J. C., & Doney, S. C. (1994). Oceanic vertical mixing: A review and a model with a nonlocal boundary layer parameterization [Journal Article]. *Reviews of Geophysics*, *32*(4), 363-403. Retrieved from http://dx.doi.org/10.1029/94RG01872 doi: 10.1029/94RG01872

Mahowald, N. M., Engelstaedter, S., Luo, C., Sealy, A., Artaxo, P., Benitez-Nelson, C., ... Siefert, R. L. (2009). Atmospheric iron deposition: Global distribution, variability, and human perturbations [Journal Article]. *Annual Review of Marine Science*, *1*(1), 245-278. Retrieved from http://www.annualreviews.org/doi/abs/10.1146/annurev.marine.010908.163727 doi: doi:10.1146/annurev.marine.010908.163727

Mahowald, N. M., Scanza, R., Brahney, J., Goodale, C. L., Hess, P. G., Moore, J. K., & Neff, J. (2017). Aerosol deposition impacts on land and ocean carbon cycles [Journal Article]. *Current Climate Change Reports*, *3*(1), 16-31. Retrieved from https://doi.org/10.1007/s40641-017-0056-z doi: 10.1007/s40641-017-0056-z

Marshall, J., Adcroft, A., Hill, C., Perelman, L., & Heisey, C. (1997). A finite-volume, incompressible navier stokes model for studies of the ocean on parallel computers [Journal Article]. *Journal of Geophysical Research: Oceans*, *102*(C3), 5753-5766. Retrieved from http://dx.doi.org/10.1029/96JC02775 doi: 10.1029/96JC02775

Marshall, J., Hill, C., Perelman, L., & Adcroft, A. (1997). Hydrostatic, quasi-hydrostatic, and nonhydrostatic ocean modeling [Journal Article]. *Journal of Geophysical Research: Oceans*, *102*(C3), 5733-5752. Retrieved from http://dx.doi.org/10.1029/96JC02776 doi: 10.1029/96JC02776

Mawji, E., Schlitzer, R., Dodas, E. M., Abadie, C., Abouchami, W., Anderson, R. F., ... others (2015). The geotraces intermediate data product 2014 [Journal Article]. *Marine Chemistry*, *177, Part 1*, 1-8. Retrieved from http://www.sciencedirect.com/science/article/pii/S0304420315000997 doi: http://dx.doi.org/10.1016/j.marchem.2015.04.005

Moffett, J. W., Vedamati, J., Goepfert, T. J., Pratihary, A., Gauns, M., & Naqvi, S. W. A. (2015). Biogeochemistry of iron in the arabian sea. *Limnology and Oceanography*, *60*(5), 1671-1688. Retrieved from https://aslopubs.onlinelibrary.wiley.com/doi/abs/10.1002/lno.10132 doi: 10.1002/lno.10132

Moore, C. M., Mills, M. M., Arrigo, K. R., Berman-Frank, I., Bopp, L., Boyd, P. W., ... Ulloa, O. (2013). Processes and patterns of oceanic nutrient limitation [Journal Article]. *Nature Geosci*, *6*(9), 701-710. Retrieved from http://dx.doi.org/10.1038/ngeo1765 doi: 10.1038/ngeo1765http://www.nature.com/ngeo/journal/v6/n9/abs/ngeo1765.html#supplementary-information

Nishioka, J., Obata, H., & Tsumune, D. (2013). Evidence of an extensive spread of hydrothermal dissolved iron in the indian ocean [Journal Article]. *Earth and Planetary Science Letters*, *361*, 26-33. Retrieved from http://www.sciencedirect.com/science/article/pii/S0012821X12006589 doi: http://dx.doi.org/10.1016/j.epsl.2012.11.040

Pham, A. L. D., & Ito, T. (2018). Formation and maintenance of the geotraces subsurface-dissolved iron maxima in an ocean biogeochemistry model [Journal Article]. *Global Biogeochemical Cycles*, *32*(6), 932-953. Retrieved from https://doi.org/10.1029/2017GB005852 doi: 10.1029/2017GB005852

Pham, A. L. D., & Ito, T. (2019). Ligand binding strength explains the distribution of iron in the north atlantic ocean [Journal Article]. *Geophysical Research Letters*, *46*(13), 7500-7508. Retrieved from https://agupubs.onlinelibrary.wiley.com/doi/abs/10.1029/2019GL083319 doi: 10.1029/2019gl083319

Riegman, R., Stolte, W., Noordeloos, A. A. M., & Slezak, D. (2000). Nutrient uptake and alkaline phosphatase (ec 3:1:3:1) activity of emiliania huxleyi (prymnesiophyceae) during growth under n and p limitation in continuous cultures [Journal Article]. *Journal of Phycology*, *36*(1), 87-96. Retrieved from https://doi.org/10.1046/j.1529-8817.2000.99023.x doi: 10.1046/j.1529-8817.2000.99023.x

Schlitzer, R., Anderson, R. F., Dodas, E. M., Lohan, M., Geibert, W., Tagliabue, A., ... others (2018). The geotraces intermediate data product 2017 [Journal Article]. *Chemical Geology*. Retrieved from http://www.sciencedirect.com/science/article/pii/S0009254118302961 doi: https://doi.org/10.1016/j.chemgeo.2018.05.040

Sharples, J., Middelburg, J. J., Fennel, K., & Jickells, T. D. (2017). What proportion of riverine nutrients reaches the open ocean? [Journal Article]. *Global Biogeochemical Cycles*, *31*(1), 39-58. Retrieved from https://doi.org/10.1002/2016GB005483 doi: 10.1002/2016GB005483

Somes, C. J., Landolfi, A., Koeve, W., & Oschlies, A. (2016). Limited impact of atmospheric nitrogen deposition on marine productivity due to biogeochemical feedbacks in a global ocean model [Journal Article]. *Geophysical Research Letters*, *43*(9), 4500-4509. Retrieved from https://doi.org/10.1002/2016GL068335 doi: 10.1002/2016GL068335

Stramma, L., Schmidtko, S., Levin, L. A., & Johnson, G. C. (2010). Ocean oxygen minima expansions and their biological impacts [Journal Article]. *Deep Sea Research Part I: Oceanographic Research Papers*, *57*(4), 587-595. Retrieved from http://www.sciencedirect.com/science/article/pii/S0967063710000294 doi: https://doi.org/10.1016/j.dsr.2010.01.005

Tagliabue, A., Aumont, O., DeAth, R., Dunne, J. P., Dutkiewicz, S., Galbraith, E., ... Yool, A. (2016). How well do global ocean biogeochemistry models simulate dissolved iron distributions? [Journal Article]. *Global Biogeochemical Cycles*, *30*(2), 149-174. Retrieved from http://dx.doi.org/10.1002/2015GB005289 doi: 10.1002/2015GB005289

Tagliabue, A., Bowie, A. R., Boyd, P. W., Buck, K. N., Johnson, K. S., & Saito, M. A. (2017). The integral role of iron in ocean biogeochemistry [Journal Article]. *Nature*, *543*(7643), 51-59. Retrieved from http://dx.doi.org/10.1038/nature21058 doi: 10.1038/nature21058

Twining, B. S., Rauschenberg, S., Baer, S. E., Lomas, M. W., Martiny, A. C., & Antipova, O. (2019). A nutrient limitation mosaic in the eastern tropical indian ocean [Journal Article]. *Deep Sea Research Part II: Topical Studies in Oceanography*, *166*, 125-140. Retrieved from http://www.sciencedirect.com/science/article/pii/S096706451830300X doi: https://doi.org/10.1016/j.dsr2.2019.05.001

Völker, C., & Tagliabue, A. (2015). Modeling organic iron-binding ligands in a three-dimensional biogeochemical ocean model [Journal Article]. *Marine Chemistry*, *173*, 67-77. Retrieved from http://www.sciencedirect.com/science/article/pii/S0304420314002229 doi: http://dx.doi.org/10.1016/j.marchem.2014.11.008

Wang, W.-L., Moore, J. K., Martiny, A. C., & Primeau, F. W. (2019). Convergent estimates of marine nitrogen fixation [Journal Article]. *Nature*, *566*(7743), 205-211. Retrieved from https://doi.org/10.1038/s41586-019-0911-2 doi: 10

.1038/s41586-019-0911-2

Ye, Y., & Völker, C. (2017). On the role of dust-deposited lithogenic particles for iron cycling in the tropical and subtropical atlantic [Journal Article]. *Global Biogeochemical Cycles*, *31*(10), 1543-1558. Retrieved from `http://dx.doi.org/10.1002/2017GB005663` doi: 10.1002/2017GB005663